# Continuous Nonlinear Model Predictive Current Control of PWM AC/DC Rectifier

Imad Merzouk[1], Noureddine Bessous[2], Mohamed Mounir Rezaoui[1*], Mohamed Elbar[1], Khansa Bdiria[1]

[1] *LAADI, Faculty of Science and Technology, University of Djelfa 17000 DZ, ALGERIA*
[2] *Faculty of Science and Technology, University of El Oued 39000 DZ, ALGERIA*

*Email[*]: mm_rezaoui@yahoo.fr*

**Abstract** –*The present work applies a nonlinear model predictive current control (NLMPCC) approach to ac/dc pulse width modulation (PWM) rectifier. A cascade structure is used to regulate Dc-link voltage and grid currents. The outer loop objective is to regulate the Dc-link voltage to the desired value, providing the level of the required active power to be used with the reactive power to calculate the referencing current for the inner loop. In the inner loop, the proposed approach is considered. After that, the nonlinear model of the converter is developed, based on continuous minimization of predicted tracking errors, the voltage at the terminal of the converter is deduced. After that, a PWM block is used to generate gate signals. Simulation results are performed to illustrate the efficiency of the proposed control law.*

**Keywords**: *AC/DC PWM rectifier, Active and reactive power, Nonlinear predictive control, Taylor approximation, Continuous minimization.*

## I. Introduction

In recent years, AC/DC pulse width modulation (PWM) converters have had more and more applications. These converters have been utilized in high voltage direct current (HVDC) transmission systems, microgrids (MG), renewable energy, and battery energy storage systems. They offer many advantages including low harmonic current distortion, bidirectional power flow, flexible control power flows, smooth and controllable dc-link voltage, high efficiency, and reliability [1-4]. To control the AC/DC PWM rectifier many strategies were proposed in the literature. Voltage oriented control (VOC) and direct power control (DPC) are initially used. The VOC reposed on double cascading loops control, the outer control loop gives the required dc-link voltage and the inner control loop controls the currents. PI regulator is used to regulate dc-ink voltage and current [5, 6]. The DPC concept regulates the active and reactive power directly based on the orientation of selected vectors from a look-up table [7, 8]. Each method has its benefits and drawback. However, both methods do not take into account the nonlinearity of the PWM ac/dc converter,

therefore they lack disturbance rejection capability and have a slow transient behavior [9-11]. For better performance of PWM ac/dc rectifier, several nonlinear control design approaches have been applied in the last decade [12, 13]. Some of these techniques are based on replacing the PI regulator in VOC control with a nonlinear controller, such as sliding mode and fuzzy controllers [14-20]. Having, as an advantage, robustness with respect to parameters variations, generalized predictive control (GPC) of a linear system is an advanced technique widely adopted to control power electronics converters recently [21-26]. Significant effort has been devoted to extend GPC to nonlinear systems, where a nonlinear optimization problem must be solved online with computational complexity. To avert this, several nonlinear predictive laws have been developed in [27, 28]. In this case, the prediction of tracking error is obtained using, Taylor expansion model of the system and the reference signal. The control law is then established by minimizing a continuous quadratic function of the tracking [29-33].

In this paper, a nonlinear predictive current control

scheme is proposed to control the ac/dc PWM converter to benefit from the high accuracy, system stability, rapidity, and constraint capability. After developing the nonlinear model of the converter, the future values of the DQ-axis currents are determined using the Taylor approximation. After that, the control law (in our case the voltages at the input of the converter) is established by minimizing a continuous quadratic function of the tracking error between referencing and measured current. Finally, a PWM block is used to calculate the switching function to be applied in semiconductor devices. The referencing currents are deduced from the required active and reactive powers, in some applications the active power is deduced from an outer control loop that regulates the level of dc-link voltage.

## II. System Modeling

Depending on the structure of the PWM converter shown in Figure 1 and using Park transformation we find a mathematical model in DQ rotating coordinate frame of ac side of PWM converter as follows:

$$\begin{cases} L\dfrac{di_d}{dt} = e_d - Ri_d + \omega Li_q - v_d \\ L\dfrac{di_q}{dt} = e_q - Ri_q + \omega Li_d - v_q \end{cases} \quad (1)$$

Where:

- $e_d, e_q$ : Source voltage in the rotating frame.
- $v_d, v_q$ : Converter terminals voltage in the rotating frame.
- $i_d, i_q$ : Line current in the rotating frame.
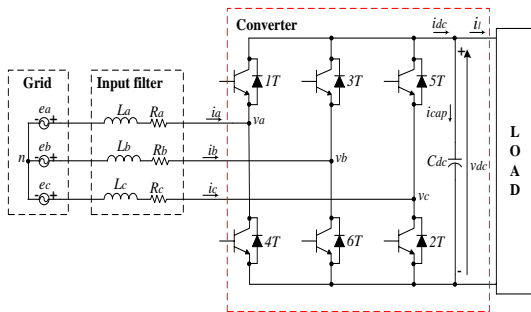- $L, R$ : Input filter inductance and resistance.



Figure 1. Topology of ac/dc rectifier

The dc-side voltage dynamics of the converter is presented by (2)

$$c\frac{dv_{dc}}{dt} = i_{dc} - i_l \quad (2)$$

Neglecting the losses in the input filter and semiconductor devices, the ac side active power is equal to dc side one, so:

$$P_{in} = \frac{3}{2}\left(e_d i_d + e_q i_q\right) = P_{out} = v_{dc} i_{dc} \quad (3)$$

Replacing (3) in (2) the dc-link voltage dynamics

$$c\frac{dv_{dc}}{dt} = \frac{3}{2cv_{dc}}\left(e_d i_d + e_q i_q\right) - \frac{i_l}{c} \quad (4)$$

From (1) and (4) the state space of the converter model is given by.

$$\frac{d}{dt}\begin{bmatrix} i_d \\ i_q \\ v_{dc} \end{bmatrix} = \begin{bmatrix} -\dfrac{R}{L}i_d + \omega i_q \\ -\dfrac{R}{L}i_q + \omega i_d \\ \dfrac{3}{2cv_{dc}}\left(e_d i_d + e_q i_q\right) - \dfrac{i_l}{c} \end{bmatrix} + \begin{bmatrix} \dfrac{1}{L} & 0 \\ 0 & \dfrac{1}{L} \\ 0 & 0 \end{bmatrix}\begin{bmatrix} e_d - v_d \\ e_q - v_q \end{bmatrix} \quad (5$$

## III. Modeling Predictive Current Control of PWM AC/DC Converter

Consider a nonlinear system, described by:

$$\begin{cases} \dot{x} = f(x) + g(x)u \\ y(t) = h(x) \end{cases} \quad (6)$$

Where:

- $x(t) \in R^n$ : state variables vector,
- $u(t) \in R^m$ : control vector,
- $y(t) \in R^m$ : output vector,
- $f(x): R^n \to R^n$ , $g(x): R^n \to R^{n \times m}$

  and $h(x): R^n \to R^m$

  Are smooth nonlinear functions.

Assumption 1: The general nonlinear system (6) is sufficiently differentiable with respect to time to any order. This implies that the nonlinear system (6) can be approximated by its Taylor-series expansion to any specified accuracy [26, 27].

Assumption 2: All States variables are measurable.

Assumption 3: The system defined in (6) has a relative degree $r^i \le 4$

The PWM converter system of (5) can be expressed in the form of (6), where:

$$f(x) = \begin{bmatrix} -\dfrac{R}{L}i_d + \omega i_q \\[2mm] -\dfrac{R}{L}i_q + \omega i_d \\[2mm] \dfrac{3}{2cv_{dc}}(e_d i_d + e_q i_q) - \dfrac{i_l}{c} \end{bmatrix},$$

$$g(x) = \begin{bmatrix} \dfrac{1}{L} & 0 \\[1mm] 0 & \dfrac{1}{L} \\[1mm] 0 & 0 \end{bmatrix}, h(x) = \begin{bmatrix} h_1(x) \\ h_2(x) \end{bmatrix} = \begin{bmatrix} i_d \\ i_q \end{bmatrix}$$

So:

$$x = \begin{bmatrix} x_1 \\ x_2 \end{bmatrix} = \begin{bmatrix} i_d \\ i_q \end{bmatrix}, u = \begin{bmatrix} u_1 \\ u_2 \end{bmatrix} = \begin{bmatrix} e_d - v_d \\ e_q - v_q \end{bmatrix},$$

$$y(t) = \begin{bmatrix} y_1(t) \\ y_2(t) \end{bmatrix}$$

The objective of predictive control is to elaborate a control law $u$ that coincides the output $y(t)$ with the reference trajectory $y_{ref}(t)$ at the next step $(t+h), h>0$ is the prediction horizon, [26]. Therefore, the control goal is to minimize the following cost function [27]:

$$J = \tfrac{1}{2}\|y(t+h) - y_{ref}(t+h)\|_Q^2 + \tfrac{1}{2}\|u(t)\|_R^2 \quad (7)$$

Where $Q \in R^{m \times m}$ is a definite positive matrix and $R \in R^{m \times m}$ is a positive semi-definite matrix.

The vector of the relative degree of our system is the vector $r^i = (r^1 r^2)^T$ $r^j$, which is the relative degree of the $j^{th}$ element of the output. It corresponds to the first derivative of $y_j$ revealing explicitly the control input $u_j$ in the expression [25]:

$$y_j^{(r_j)} = L_f^{(r_j)} + h_j + \sum_{i=1}^{m}\left(L_{gi} L_f^{r_j - 1} h_j\right) u_i \quad (8)$$

After calculation, we find that $r^1 = r^2 = 1$

A simple way to predict the influence of $u(t)$ on $y(t+h)$ is to expand it in the $r = (r^1 r^2)^T = (1\ 1)^T$ order Taylor series [31].

$$y(t+h) = y(t) + \begin{bmatrix} hL_f h_1(x) \\ hL_f h_2(x) \end{bmatrix} + \begin{bmatrix} h & 0 \\ 0 & h \end{bmatrix}\begin{bmatrix} L_{g1} h_1(x) \\ L_{g1} h_2(x) \end{bmatrix} \quad (9)$$

**Assumption 4:** For the output $y(t)$ of the nonlinear system (6) to follow the reference trajectory $y_{ref}(t)$, we assume that the last one is $r^i$ differentiable (is differentiable $r^i$ times). This condition ensures the controllability of the output along with the setpoint $y_{ref}(t)$ [26].

Therefore we can apply the Taylor expansion of order $r = (r^1 r^2)^T = (1\ 1)^T$ to the reference signal:

$$y_{ref}(t+h) = y_{ref}(t) + \begin{bmatrix} h\dot{y}_{ref\,1} \\ h\dot{y}_{ref\,2} \end{bmatrix} \quad (10)$$

With: $y_{ref}(t) = \begin{bmatrix} y_{ref\,1}(t) \\ y_{ref\,2}(t) \end{bmatrix}$

By replacing equations (9) and (10) in (7) the cost function is then written as:

$$J = \frac{1}{2}\left\| \begin{aligned} e(t) + \begin{bmatrix} hL_f h_1(x) \\ hL_f h_2(x) \end{bmatrix} - \begin{bmatrix} h\dot{y}_{ref\,1} \\ h\dot{y}_{ref\,1} \end{bmatrix} \\ + \begin{bmatrix} h & 0 \\ 0 & h \end{bmatrix}\begin{bmatrix} L_{g1} h_1(x) \\ L_{g1} h_1(x) \end{bmatrix} u \end{aligned} \right\|_Q^2 + \frac{1}{2}\|u(t)\|_R^2 \quad (11)$$

Where:

$e(t)$ is the tracking error given as,

$e(t+h) = y(t+h) - y_{ref}(t+h)$

The optimal solution is then obtained by minimizing the criterion (11) for the nonlinear system (6) compared to the control vector $u(t)$:

$$u(t) = -\left[\left(\begin{bmatrix} h & 0 \\ 0 & h \end{bmatrix}\begin{bmatrix} L_{g1}h_1(x) \\ L_{g1}h_2(x) \end{bmatrix}\right)^T\right]^{-1}$$
$$Q\begin{bmatrix} h & 0 \\ 0 & h \end{bmatrix}\begin{bmatrix} L_{g1}h_1(x) \\ L_{g1}h_2(x) \end{bmatrix} + R$$

$$\left(\begin{bmatrix} h & 0 \\ 0 & h \end{bmatrix}\begin{bmatrix} L_{g1}h_1(x) \\ L_{g1}h_2(x) \end{bmatrix}\right)^T \qquad (12)$$

$$Q\left[e(t) + \begin{bmatrix} hL_f h_1(x) \\ hL_f h_2(x) \end{bmatrix} - \begin{bmatrix} h\dot{y}_{ref1} \\ hh\dot{y}_{ref2} \end{bmatrix}\right]$$

With:

$$\begin{bmatrix} hL_f h_1(x) \\ hL_f h_1(x) \end{bmatrix} = \begin{bmatrix} h\left(-\dfrac{R}{L}i_d + \omega i_q\right) \\ h\left(-\dfrac{R}{L}i_q - \omega i_d\right) \end{bmatrix}, \begin{bmatrix} L_{g1}h_1(x) \\ L_{g1}h_2(x) \end{bmatrix} = \begin{bmatrix} \dfrac{1}{L} & 0 \\ 0 & \dfrac{1}{L} \end{bmatrix}$$

## IV. Simulations and discussion

To verify the mathematical model of the PWM rectifier and to test the efficiency of the control laws presented in this work, we will test the program numerically in the environment MATLAB / Simulink. The overall control structure is illustrated in Figure 2. The control is based on two cascading loops, the outer loop controls the level of dc-link voltage using PI regulator, and in the inner loop, the d-q axis currents are regulated using predictive control.

The converter parameters are given in Table 1. The design of the nonlinear model predictive current controller is based on the continuous model. The general control objective is to extract the switching state that allows tracking the reference current, using a cascade structure.
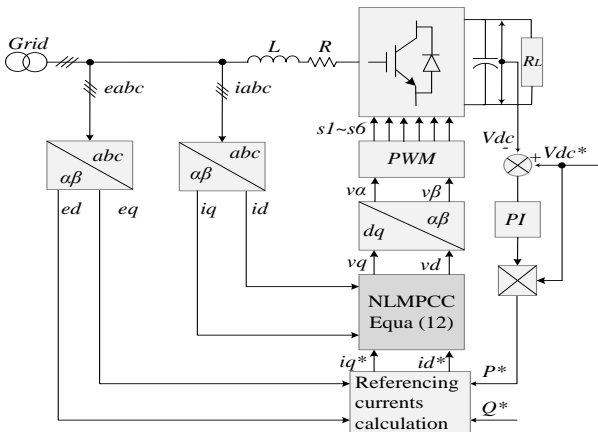


Figure 2. Control diagram of the proposed NLPC

Table 1. Power circuit parameters.

| Items | Symbol | Value |
|---|---|---|
| Input filter inductance | $L$ | 12 $mH$ |
| Input filter resistance | $R$ | 0.3 $\Omega$ |
| DC-bus capacitor | $C$ | 500μF |
| Load resistance | $RL$ | 200 $\Omega$ |

### IV.1. Case 1: Dc-Link Voltage and Reactive Power Step

When the simulation reaches a steady state, two steps are applied on the reference of DC-link voltage at t= 1.5 and the reference of reactive power at t=2s. The results are presented in Figure 3.
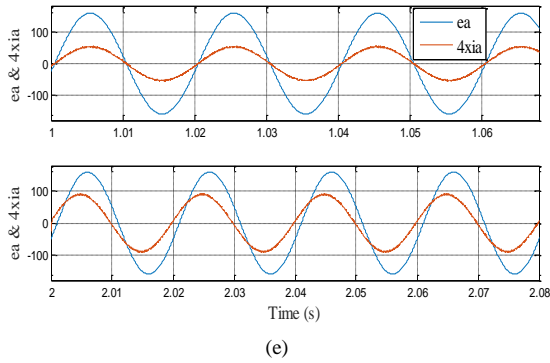


(a)



(b)



(c)



(d)

(e)
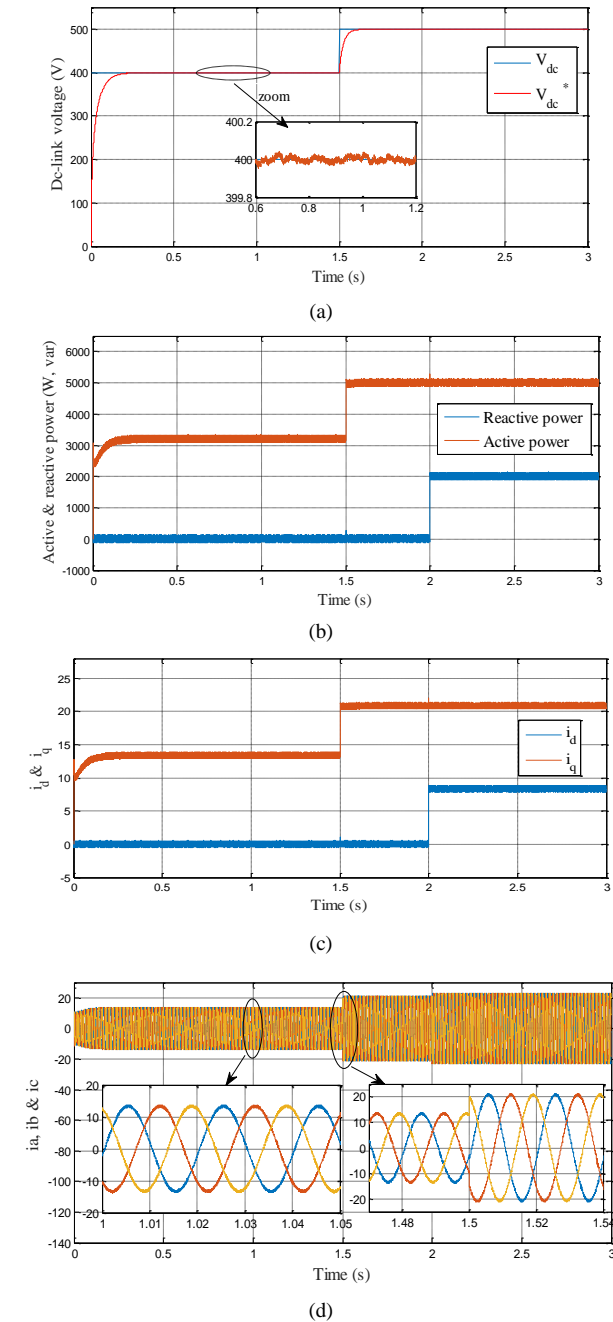
Figure 3. Simulation results of Case I: (a) Dc-link voltage, (b) Active and reactive powers, (c) Grid voltage and current, (dd) d and q-axis current, (e) Three phases current.

When the reference of Dc-link voltage boosts from 400V to 500V, the Dc-link voltage stabilizes to the new reference on approximately 0.05s as shown in Figure 3-a. With this change the active power exchanged with the grid is increased too, in order to assure the required power requested at the output of the converter as observed in Figure 3-b. However, the reactive power stays unchanged.

We can conclude from Figure 3-c that the proposed control techniques ensure a decoupled control between active and reactive power, where q-axis current controls the active power and d-axis current controls the reactive power. The transient response of the inner loop is too high. The measured current reaches the new reference immediately without overshoot.

In Figure 3-d, the three phases current is presented, the currents are sinusoidal with a THD of less than 3%. In addition, along with the rise of active power, the amplitude of currents rises too.

In Figure 3-e, both grid voltage and current are plotted in the same figure, before and after the referencing reactive power step is applied. When the reactive power is kept zero the voltage and current are in phase. But, when the reactive power increases to 1000 Var to a phase shift between the voltage and current is created. So the converter can be used as a reactive power compensator of the grid without affecting the output Dc-link voltage, or the grid current quality.

### *IV.2. Case 2: load Steps*

In this sub-section, a load step is applied at t=1s (from 60Ω to 40Ω). The dc-link voltage increases slightly and then returns to its reference without affecting the stability of the system as shown in Figure 4-a. From Figures Figure 4-b and Figure 4-c the active power, q-axis

current, and the amplitude of the line current increase smoothly to a new value without a change in reactive power.

In Figure 4-d, the three phases current is plotted; it is observed that the amplitude of the current droops to a new value, the current is always balanced and sinusoidal.
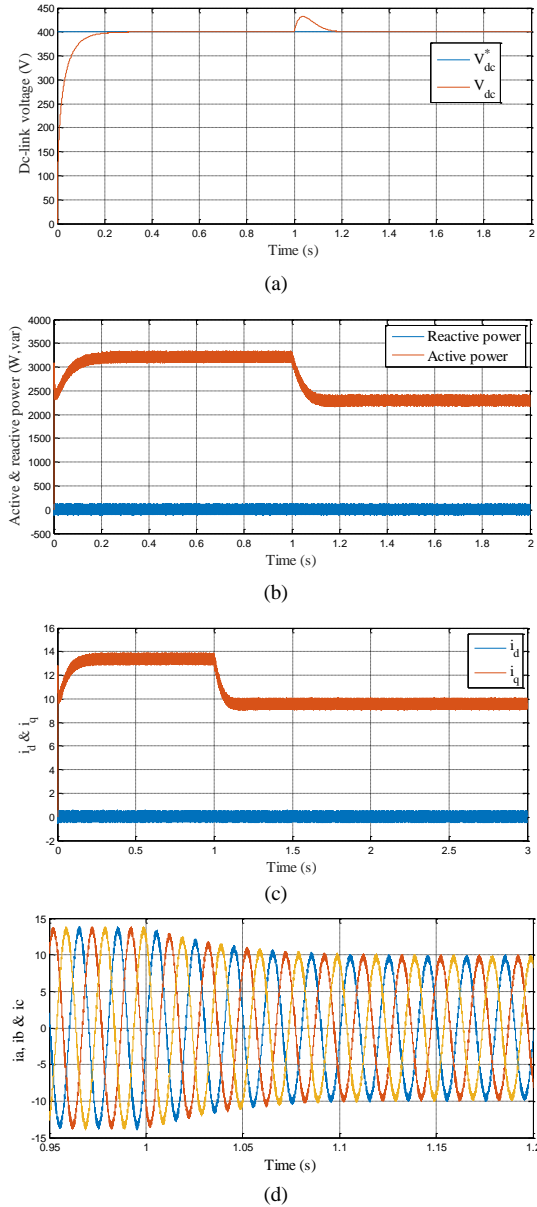


(a)



(b)



(c)



(d)

Figure 4. Simulation results of Case 2: (a) Dc-link voltage, (b) Active and reactive power, (c) d and q-axis current, (d) Three phases current.

### *IV.3. Case 3: Grid Voltage Droops*

In With the integration of renewable energy in the grid, the grid voltage may drop from time to time, so we see to test the behaviour of the converter when the grid voltage drops by 30%. The results are shown in Figure 5.

From Figure 5, the control law has a perfect transient under voltage droop. The system remains stable. An

increase in the amplitude of the current is to be considered in order to keep the system function in gat the same power level. So the average value of the active and reactive power remains unchanged, the system always works at the required Dc-link voltage with a unity power factor. The inner control loop has a very fast dynamic while keeping the system stable.
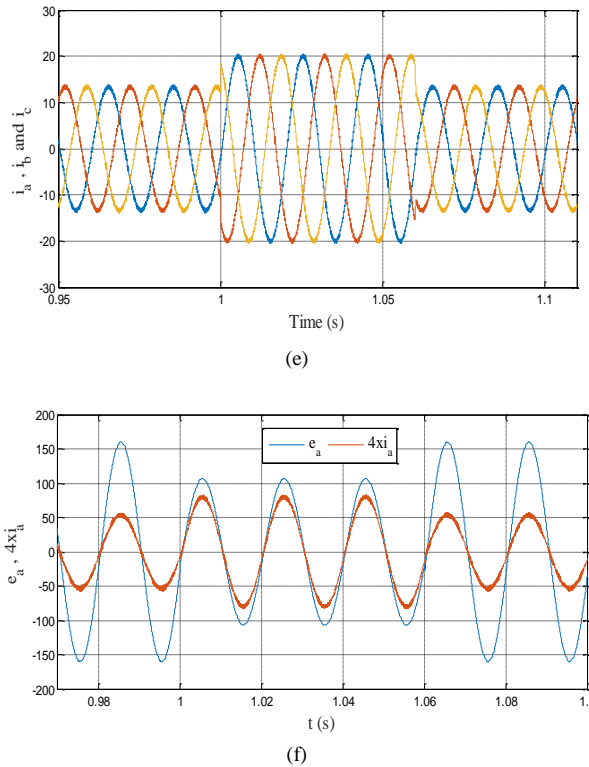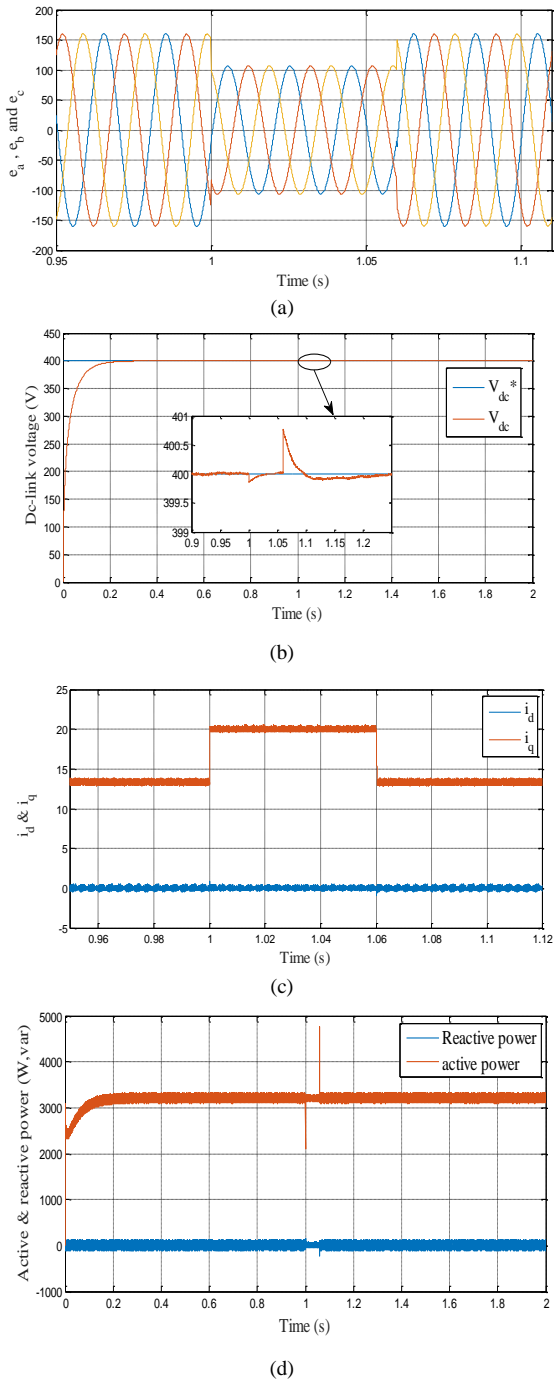


(a)



(b)



(c)



(d)



(e)



(f)

Figure 5. Simulation results of Case 3: (a) Grid voltage, (b) dc-link voltage (c) d and q-axis current, (d) Active and reactive power, (e) Grid current.

### IV.4. Case 4: Line Inductance Mismatch Investigation

To investigate the robustness of the proposed control method, a big change in input filter inductance is applied, the value of the inductance is stepped from 12 to 2 mH at t=1s and afterward, it is increased to 20 mH at t=1.5s. Slight perturbation does not exceed 1V is provoked in the dc-link voltage. Otherwise, the dc-link stays smooth and in its reference value as shown in Figure 6-a.

According to the wave forms of current in Figure 6-b, the change of the input filter inductance has no real impact on the current quality, the THD is practically unchanged. So the proposed control showed very high robustness against the system parameter mismatch.
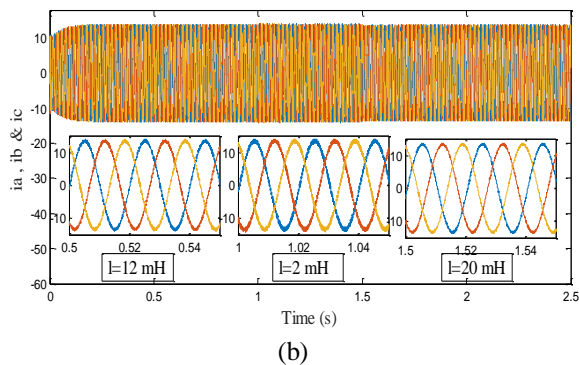


(a)

(b)
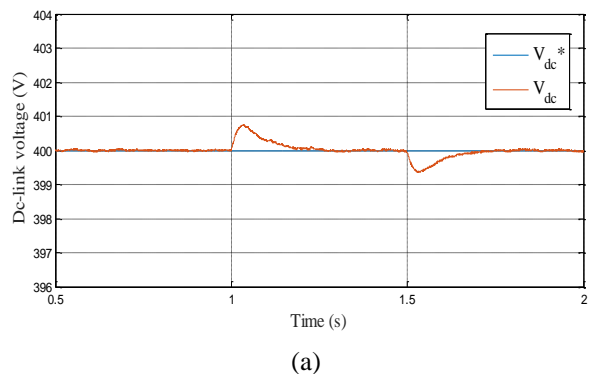
Figure 6. Simulation results of Case 4: (a) Dc-link voltage, (b) Three phases current.

# V. Conclusion

In this paper a nonlinear model predictive current control has been proposed in order to improve the transient behavior of the PWM ac/dc rectifier. The nonlinear predictive control law was extracted using Taylor expansion and by choosing the d and q-axis current as control variables. The reference of current was deduced from the required values of active and reactive powers, where the active power determines the level of dc-link voltage which is controlled by the PI regulator. The control scheme was tested under significant changes in operating points of the converter and external disturbances (source voltage and load variation). The results are encouraging where the system stayed stable and follow the recommended reference. In order to investigate the robustness of the proposed control law, a sever change in the input filter was applied. In this case, the system showed high quality results.

# References

[1] MH. Naushath, DR. Athula, MG. Aniruddha, TF. Ioni, "Investigation of fault ride-through capability of hybrid VSC-LCC multi-terminal HVDC transmission systems", IEEE Transactions on power delivery, Vol. 34, Issue. 1, 2019, pp. 241-250.

[2] G. Praveen, P. Venkata, P. Priyanka, CJ. Francis, "VACMC-based hybrid AC/LVDC micro-grid", IET Renewable Power Generation, Vol. 11, Issue. 4, 2017, pp. 521-528.

[3] IM. Moghaddam, HC. Badrul, S. Mohajeryami, "Predictive operation and optimal sizing of battery energy storage with high wind energy penetration", IEEE Transactions on Industrial Electronics, Vol. 65, Issue. 8, 2018, pp. 6686-6695.

[4] R. Katayoun, CC. Chin, Z. Rui, "Energy cooperation optimization in microgrids with renewable energy integration", IEEE Transactions on Smart Grid, Vol. 9, Issue. 2, 2018, pp. 1482-1493.

[5] V. Blasko, M. Kaura, "A new mathematical model and control of a three-phase AC-DC voltage source converter", IEEE Transactions on Power Electronics, Vol. 12, Issue. 1, 1997, pp. 116-123.

[6] M. M. Rezaoui, N. Bessous, I. Merzouk, "Control of 3x7 matrix converter with PWM three intervals Modulation", International Journal of Energetica (IJECA), Vol. 4, Issue 2, 2019, pp.14-20.

[7] K. Kulikowski, A. Sikorski, "new DPC look-up table methods for three-level AC/DC converter", IEEE Transactions on Industrial Electronics, Vol. 63, Issue. 12, 2016, pp.7930-7938.

[8] M. Imad, MLBM. Lokman, "Improved direct power control for 3-level AC/DC converter under unbalanced and/or distorted voltage source conditions", Turkish Journal of Electrical Engineering & Computer Sciences, Vol. 24, Issue. 3, 2016, pp. 1847-1862.

[9] G. Fouad, A. Abdelmajid, L. Ibtissam, C F. Zahra, "Formal framework for nonlinear control of PWM AC/DC boost rectifiers—controller design and average performance analysis", IEEE Transactions on Control Systems Technology, Vol. 18, Issue. 2, 2010, pp. 323-335.

[10] Lee DC, Lee GM, Lee KD. , "DC-bus voltage control of three-phase AC/DC PWM converters using feedback linearization", IEEE Transactions on Industry Applications, Vol. 36, Issue. 3, 2000, pp. 826-833.

[11] PK. Dashn Nayak, "Nonlinear control of voltage source converters in ac–dc power system", ISA Transaction, Vol. 53, Issue. 4, 2014, pp. 1268-1285.

[12] TS. Lee, "Input-output linearization and zero-dynamics control of three-phase AC/DC voltage-source converters", IEEE Transactions on Power Electronics, Vol. 18, Issue. 1, 2003, pp. 11-22.

[13] R. Gerasimos, CPS Carlo, "An H-Infinity feedback control approach for three-phase voltage source converters", IECON 2014 - 40th Annual Conference of the IEEE Industrial Electronics Society, Dallas, TX, USA 29 Oct.-1 Nov 2014.

[14] S. Fadia, V. Hani, YK. Hadi, M. Nazih, K. Al-haddad, "Sliding mode fixed frequency current controller design for grid-connected NPC inverter", IEEE Journal of Emerging and Selected Topics in Power Electronics, Vol. 4, Issue. 4, 2016, pp. 1397-1405.

[15] SK. Kim, "Robust output voltage tracking Algorithm for Three-phase rectifier with variable sliding surface", IET Power Electronics, Vol. 11, Issue. 6, 2018, pp.1119-1127.

[16] J. Liu, Y. Yin, W. Luo, S. Vazquez, LG. Franquelo, L. Wu , "Sliding mode control of a three-phase AC/DC voltage source converter under unknown load conditions: industry applications", IEEE Transactions on Systems, Man, and Cybernetics Systems, Vol. 48, Issue. 10, 2018, pp. 1771-1780.

[17] S. Dan, W. Xiaohe, F. Yang, "Backstepping direct power control without phase-locked loop of AC/DC converter under both balanced and unbalanced grid conditions",

IET Power Electronics, Vol. 9, Issue. 8, 2016, pp. 1614-1624.

[18] C. Cecati, A. Dell'Aquila, A. Lecci, M. Liserre, "Implementation issues of a fuzzy-logic-based three phase active rectifier employing only voltage sensors",. IEEE Transactions on Industrial Electronics, Vol. 52, Issue. 2, 2005, pp. 378-385.

[19] A. Hakan, O. Fatih Kececioglu, A. Gani, C. Yildiz, S. Mustafa, "Improved control configuration of PWM rectifiers based on neuro-fuzzy controller", Springer Plus. 2016; 5:1142.

[20] J. Rodríguez, PC. Estay, "Predictive control of power converters and electrical drives", (Wiley, Chichester, West Sussex, UK; Hoboken, N.J.; 2012).

[21] AY. Hector, AP. Marcelo, J. Rodriguez, "Analysis of finite-control-set model predictive current control with model parameter mismatch in a three-phase inverter", IEEE Transactions on Industrial Electronics, Vol. 63, Issue. 5, 2016, pp. 3100-3107.

[22] XL. Dan, WZ. Peng , "Improved finite-control-set model predictive control for active front-end rectifiers with simplified computational approach and on-line parameter identification", ISA Transaction. 2017; 69: pp. 51-64.

[23] XY. Xing, C. Zhang, J. He, A. Chen, Z. Zhang, "Model predictive control for parallel three- level T-type grid-connected inverters in renewable power generations", IET Renewable Power Generation, Vol. 11, Issue. 11, 2017, pp. 1353-1363.

[24] P. Falkowski, A. Sikorski, "Finite control set model predictive control for grid-connected AC-DC converters with LCL filter". IEEE Transactions Industrial Electronics, Vol. 65, Issue. 4, 2018, pp. 2844-2852.

[25] T. He, lu D. Dah-chuan , L. Li, J. Zhang, L. Zheng, J. Zhu, "Model-predictive sliding-mode control for three-phase AC/DC converters", IEEE Transactions on Power Electronics, Vol. 33, Issue. 10, 2018, pp. 8982-8993.

[26] L. Ping, "Non linear predictive control of continuous nonlinear systems", Journal of Guidance, control and dynamics, Vol. 17, Issue. 3, 1994, pp. 553-560.

[27] SN. Singh, M. Steinberg, RD. Digirolamo, "Nonlinear predictive control of feedback linearizable systems and flight control system design", Journal of Guidance, control and dynamics, Vol. 18, Issue. 5, 1995, pp. 1023-1028.

[28] J. Corriou, "Process Control: Theory and Applications", Springer 2017. Book ISBN: 978-1-84996-911-6.

[29] K. Bdirina, MS. Boucherit, R. HEDJAR, D. DJOUDI, NAIMI H. Non linear predictive control with input constraints of electrical wheelchair", The Mediterranean Journal of Measurement and Control, Vol. 10, Issue. 2, 2014, pp. 215-223.

[30] L. Tao, W. Tan, G. Chen, D. KONG, "A novel robust model predictive controller for aerospace three-phase PWM rectifiers", Energies. 2018; 11: 2490.

[31] E. Rachid, SM. Muyeen, A. Al-Durra, S. Leng, "Experimental validation of a robust continuous nonlinear model predictive control based grid-interlinked photovoltaic inverter", IEEE Transactions on Industrial Electronics, Vol. 63, Issue. 7, 2016, pp. 4495-4505.

[32] A. Berboucha, K. Djermouni, K. Ghedamsi, D. Aouzellag, "Fuzzy logic control of wind turbine storage system connected to the grid using multilevel inverter", International Journal of Energetica (IJECA), Vol 2. Issue. 1, 2017, pp.15-23.

[33] Y. Saidi, A. Mezouar, Y. Miloud, M. A. Benmahdjoub, M. Yahiaoui, "Fuzzy Logic Based Robust DVC Design of PWM Rectifier Connected to a PMSG WECS under wind/load Disturbance Conditions", International Journal of Energetica (IJECA), Vol. 4, Issue 1, 2019, pp.37-43.